



## **EVALUATION OF NATURAL RADIOACTIVITY IN BEACH SANDS OF THE GUANABARA BAY**

**Azevedo, Ary M.<sup>1</sup>, Lopes, Thomaz J.<sup>1</sup>, Salazar, Augilmar P.<sup>1</sup>, Silveira, Paulo C.R. P.<sup>1</sup>,  
Batista, Joana S.<sup>1</sup>, Ferreira, Victor A.V.<sup>1</sup>, Nunes, Wallace V.<sup>1</sup>, Cardoso, Domingos D.O.<sup>1</sup>**

<sup>1</sup> Instituto Militar de Engenharia, 22290-270, Urca, Rio de Janeiro, Brasil.  
ary@ime.eb.br

**Keywords:** NORM, Guarapari Beach, Guanabara Bay, Monazite Sand

### **ABSTRACT**

Due to ocean currents, monazite sand from Guarapari beach may be transported to beaches around Guanabara Bay in Rio de Janeiro. It was found that among the beaches analyzed, those on Ilha do Governador did not detect monazite sand, but other radionuclides were detected and will be analyzed later.

### **1. INTRODUCTION**

The increase in exposure to natural radiation can occur due to the elevated concentration of radioisotopes in the soil. In the region around Guanabara Bay, this increase is mainly due to the presence of monazite sand, composed of thorium, uranium, potassium and consequently their radioactive daughters like, Ra-226 and Ra-228 [1], [2]. This sand is classified as NORM – Naturally Occurring Radioactive Materials, and its presence can lead to increased natural radiation exposure to the population [3], [4]. Since the dynamics of sand transport are influenced by climatological and oceanographic factors, the anomaly of natural radioactivity found on beaches in the state of Espírito Santo may occur and/or be transported to sands on other Brazilian beaches [5], [6]. This work continues the study published in the proceedings of the “International Joint Conference RADIO 2022” [7]. This work aimed to evaluate the presence of monazite sand on beaches around Guanabara Bay.

### **2. MATERIALS AND METHODS**

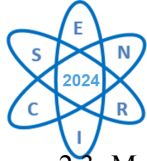
#### **2.1. Sample Screening**

For this work, in situ screening of beach sands in the cities of Rio de Janeiro and Niterói was conducted. This screening consisted of verifying the exposure dose rate of bathers, adopting a background (BG) value of 0.14  $\mu\text{Sv/h}$ , and collecting samples from beaches that exceeded this value for laboratory analysis.

These measurements were made with the Radeye-PRD detector, lent by the nuclear engineering department of IME. The RadEye-PRD detector use a small photomultiplier. This detector has a lower level detection (LLD) from 0.01 to 250  $\mu\text{Sv/h}$  [8].

#### **2.2. Sample Preparation**

The only preparation done was weighing the sample, adopting a weight of 50 g of sand per test. This test was conducted to simulate the real condition of bathers. The gamma spectroscopy was measured on April 2022. However, as the process of transporting particulates through marine currents is slow, it can be considered that the results obtained in this work are relevant today. [9]–[11].



### 2.3. Measurements with Spir-ID

The gamma spectrum of the samples and the background radiation was taken for 1 hour (3600 seconds) of live time, with Spir-ID detector [12]. The results presented are the net spectra of the samples [7]. This detector was used because NaI(Tl) crystals are used as a reference in the class of inorganic scintillator detectors [13].

Samples were also analyzed using a BGO detector [14] to compare with results obtained from the Spir-ID detector [12]. Some information about the detectors is described in Table 1 [15].

Material	Scintillation Efficiency (%)	Decay ( $\mu s$ )	Density ( $gcm^{-3}$ )
NaI(Tl)	100	0.23	3.67
BGO	8	0.30	7.13

Table 1. Characteristics of detectors used

This detector has a 3" crystal and uses a photomultiplier. The Spir-ID detector has an Lower Level Detection (LLD) from 0.001 to 9999  $\mu Sv/h$ . This equipment has an auto-calibration system and uses a low-activity cesium-137 source [12].

For the measurement of the samples, a collimated arrangement was adopted [16].

### 2.4. Measurements with BGO

Despite the intrinsic characteristics of the detector described in Table 1, the detector BGO [15], this detector was used due to its higher density and the model used being equipped with a photodiode array [14]. The gamma spectrum of the samples and the background radiation was taken for 1 day (84600 seconds) of live time. The results presented are the net spectra of the samples. This detector was energy-calibrated with a cesium-137 source, adopting a collimated experimental arrangement [16].

## 3. RESULTS AND DISCUSSION

### 3.1. *In Situ* Measurement Results

The beaches that exceeded the BG limit are located in the city of Rio de Janeiro, in the neighborhoods of Urca, Leme, and Ilha do Governador, and in the city of Niterói. The beaches are positioned as shown in Figure 1

The beaches in the city of Rio de Janeiro were: (1) Leme Beach, (2) Red Beach, (3) Urca Beach, (4) Ribeira Beach, (5) Bica Beach, (6) Guanaba Beach

The beaches in Niterói were: (7) Ferry embarkation point, (8) São Francisco Beach, (9) Charistas Beach, (10) Jurujuba Beach.

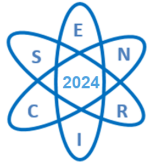


Figure 1. Map of analyzed beaches

### 3.2. Spir-ID Detector Measurement Results

Figure 2 shows the gamma spectrum taken from Red Beach.

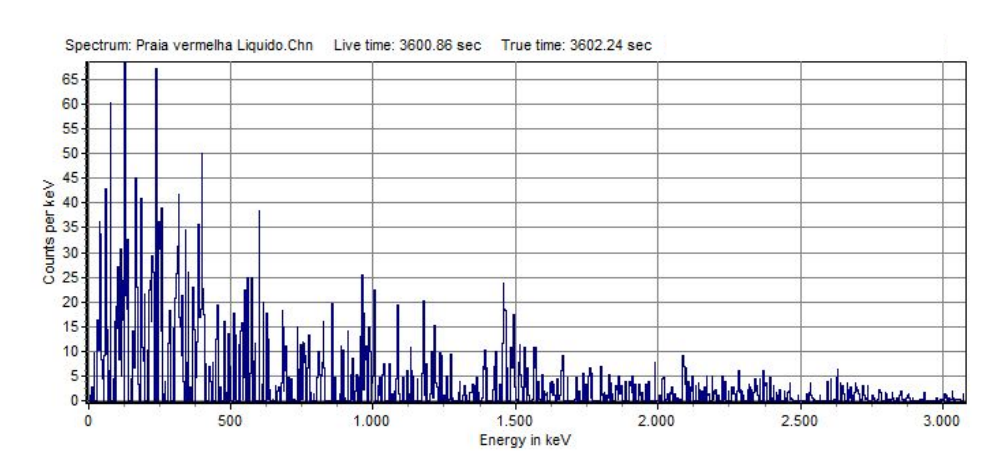
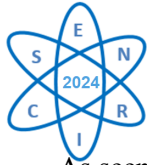


Figure 2. Net Spectrum of Red Beach measured if Spir-ID



As seen in Figure 2, the Spir-ID detector did not identify any characteristic photopeaks. Only this result was included because the Spir-ID detector did not present any characteristic photopeaks in the other samples.

### 3.3. BGO Detector Results

As can be seen in the figures below, the number of counts in the region below 200 keV was elevated, indicating that the BGO detector was effective in measuring the gamma emitted by the radionuclides present.

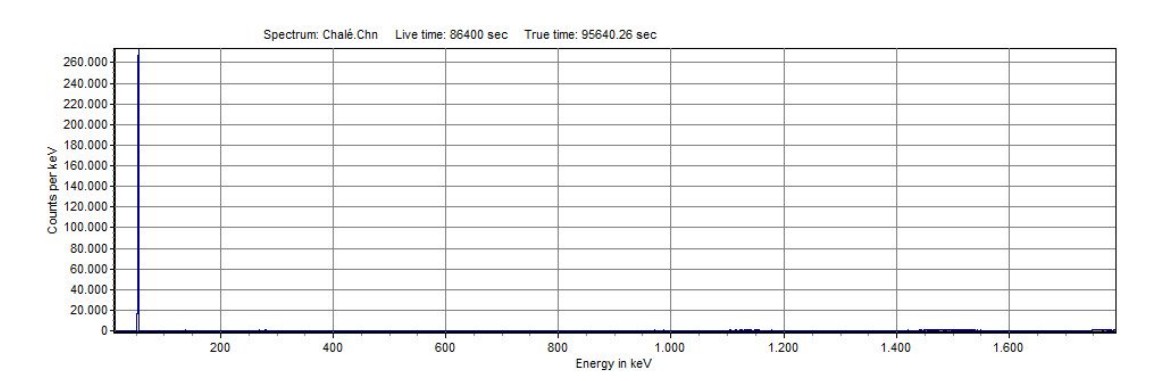


Figure 3. net gamma spectrum of Chale Beach Measured if BGO

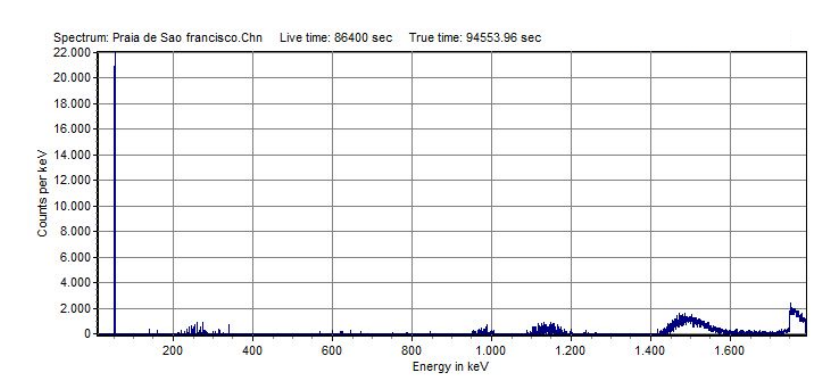


Figure 4. net gamma spectrum of São Francisco Beach Measured if BGO

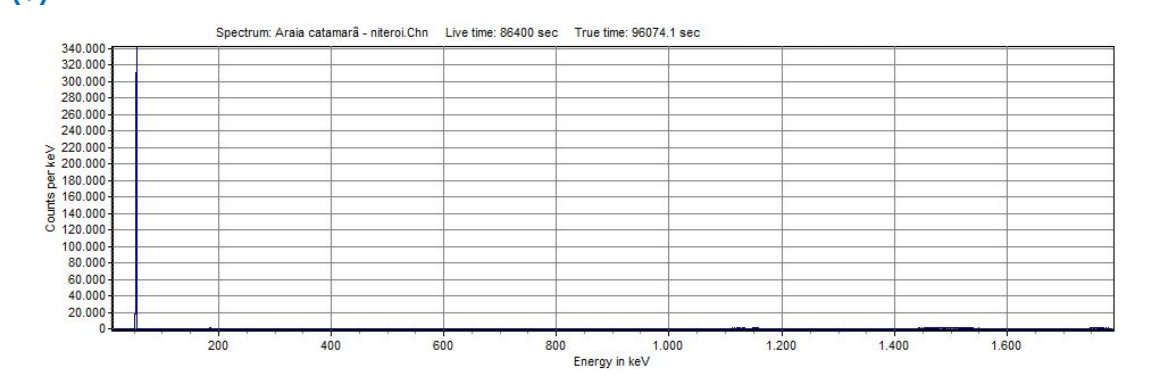
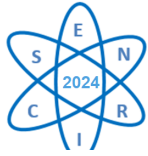


Figure 5. net gamma spectrum of Ferry embarkation point Beach Measured if BGO

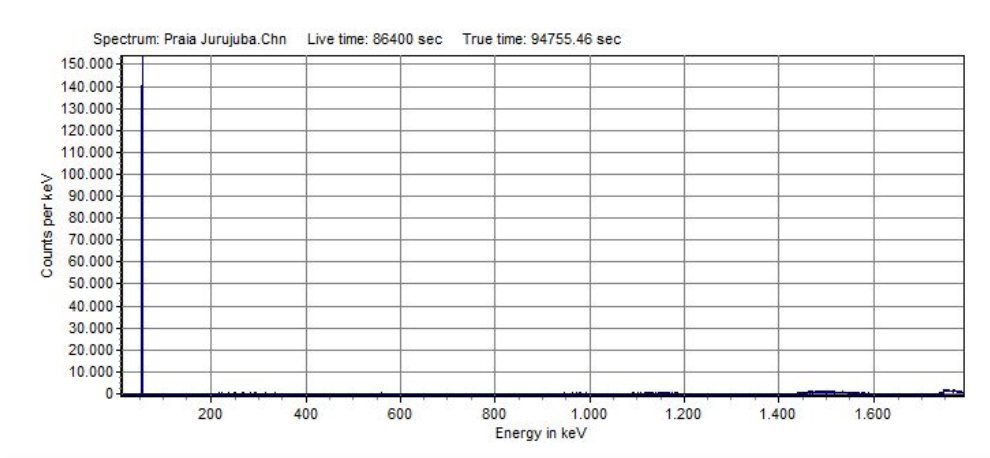


Figure 6. net gamma spectrum of Jurujuba Beach Measured if BGO

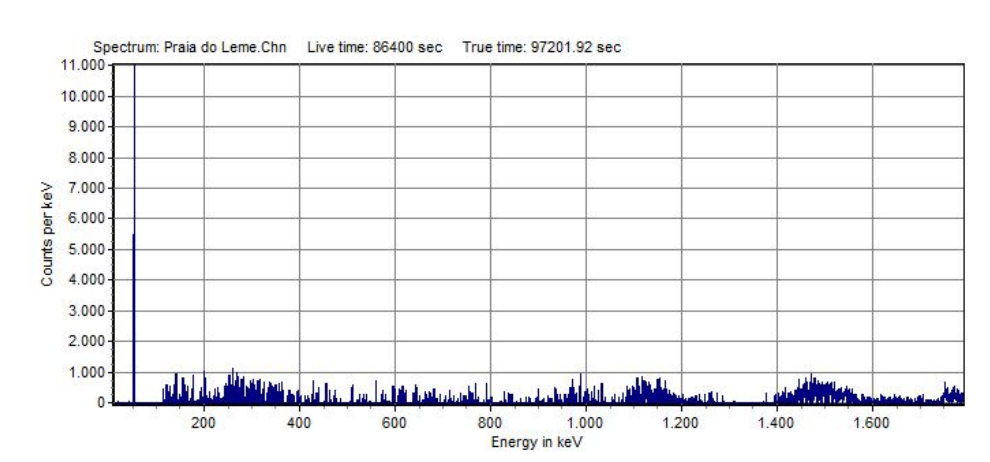


Figure 7. net gamma spectrum of Leme Beach Measured if BGO

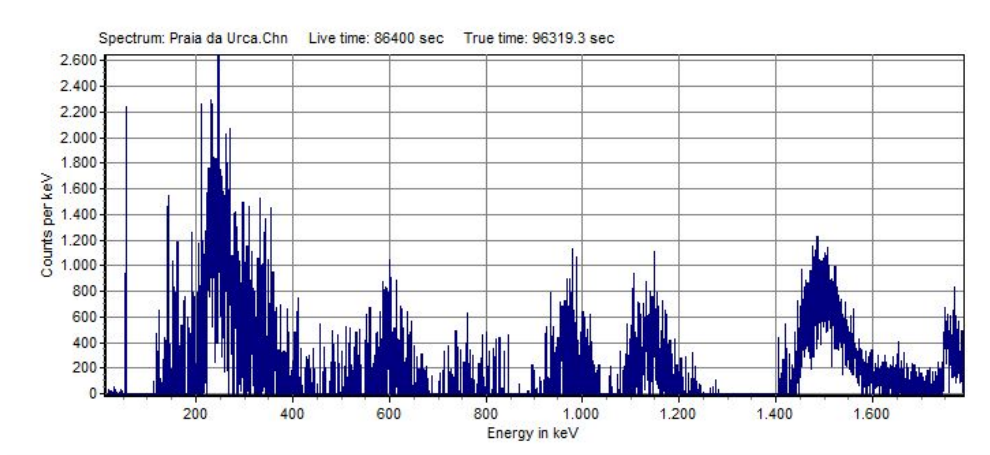
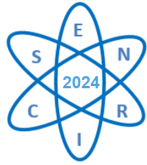


Figure 8. net gamma spectrum of Urca Beach Measured if BGO

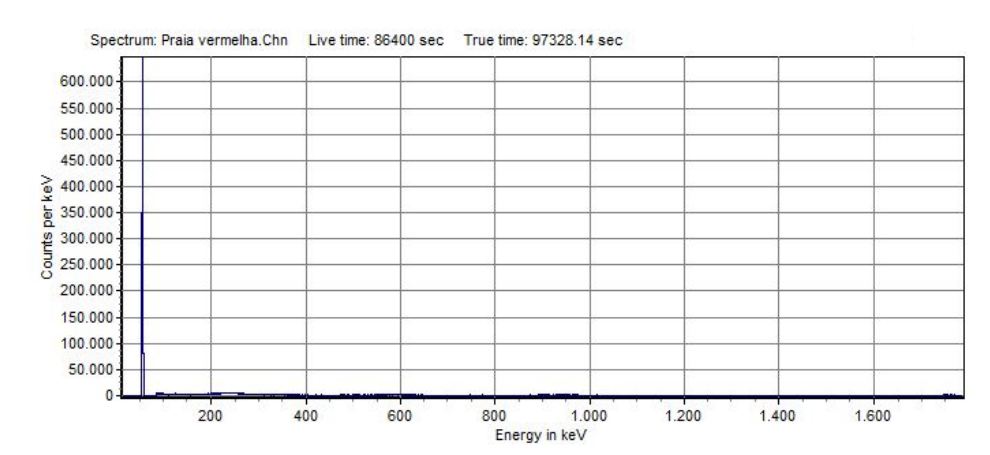


Figure 9. net gamma spectrum of Red Beach Measured if BGO

### 3.4. Discussion of Results

One explanation lies in the measurement methodology of the detectors. The Radeye-PRD generates the electronic pulse through a photodiode array and has a faster response time. Despite this better efficacy, the Radeye detector does not perform energy spectrum surveys. Another possible hypothesis is the measured concentration. In the in situ measurement, the concentration of nuclear material is higher, causing more pulses to be generated in the Radeye-PRD detector.

It is not possible to compare the results obtained by the Spir-ID and BGO due to the change in methodology employed for each detector. However, it can be stated that the BGO detector proved efficient for detecting low-activity and low-energy sources.

By analyzing the gamma spectra generated by the BGO from the beaches: Charitas (Figure 3), São Francisco (Figure 4), the ferry embarkation area in Niterói (Figure 5), Jurujuba (Figure 6), Leme



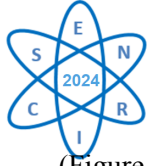


(Figure 7), Urca (Figure 8), and Red Beach (Figure 9), a higher count at low energy was observed, contributing to the hypothesis of possible contamination of the analyzed beaches by ocean currents linking Guarapari beach in Espírito Santo to Guanabara Bay in Rio de Janeiro.

#### 4. CONCLUSION

The BGO detector proved effective for measuring low-energy and low-activity sources. This is due to its high density and low light efficiency compared to NaI(Tl), and the photodiode array employed in this detector.

Due to its intrinsic efficiency, the BGO detector demonstrated to be an alternative for detecting low-activity and low-energy sources. One of its possible applications is in screening for the detection of NORM material in potentially contaminated materials.

From the analysis of the spectra measured by the BGO detector, it can be concluded that the beaches on Ilha do Governador (Guanabara Beach, Ribeira Beach, and Bica Beach) did not show significant counts related to monazite sand. However, other radionuclides were detected. The other samples had relevant counts in the low-energy region, representing *NORM* material.

For better identification of the chemical elements present in the analyzed sands, it is suggested to conduct an X-ray fluorescence test.

#### ACKNOWLEDGMENTS

We would like to express our deepest gratitude to the Instituto Militar de Engenharia (IME), especially to the departments of Nuclear Engineering and Engineering and Materials Science, for their significant contribution to the advancement of science and technology in Brazil. The commitment and excellence of these departments have been fundamental to the development of innovative research and the training of highly qualified professionals.

Furthermore, we would like to thank the funding agencies, such as the Coordination for the Improvement of Higher Education Personnel (CAPES) and the National Institute of Studies and Educational Research Anísio Teixeira (INEP), for the financial and institutional support that made it possible to carry out our research projects and train high-level human resources.

#### References

- [1] Z. Sóti, J. Magill, and R. Dreher, “Karlsruhe nuclide chart—new 10th edition 2018”, *EPJ Nuclear Sciences & Technologies*, vol. 5, p. 6, 2019.
- [2] X. Zhu and R. O’Nions, “Monazite chemical composition: Some implications for monazite geochronology”, *Contributions to Mineralogy and Petrology*, vol. 137, no. 4, pp. 351–363, 1999.
- [3] R. R. d. Aquino, “Avaliação da radioatividade natural em areias das praias da grande vitória, espírito santo”, M.S. thesis, Universidade de São Paulo, Brasil, 2010.
- [4] L. Barcellos, P. Silveira, A. Nicolau, R. Schirru, and C. Pereira, “Dynamic prediction of spatial dose rate distribution during nuclear severe accidents by means of active machine learning and mobile sensors”, *Nuclear Engineering and Design*, vol. 414, p. 112 609, 2023.
- [5] L. F. Barros, “Avaliação da variação da radioatividade natural em areias da praia de camburi, vitória e espírito santo com fatores climatológicos e geológicos da região”, M.S. thesis, IPEN, São Paulo, SP, Brasil, 2013.
- [6] P. R. Silveira, D. d. F. Naiff, C. M. Pereira, and R. Schirru, “Reconstruction of radiation dose rate profiles by autonomous robot with active learning and gaussian process regression”, *Annals of Nuclear Energy*, vol. 112, pp. 876–886, 2018.



*Semana Nacional de Engenharia Nuclear e da Energia e Ciências das Radiações - VII SENCIR*  
*Belo Horizonte, 12 a 14 de novembro de 2024*

- [7] *Proceedings*, SBPR, Rio de Janeiro: SBPR, pp. 222–223. [Online]. Available: [https://www.sbpr.org.br/site/media/arquivos/livro\\_de\\_resumos\\_ijc\\_radio\\_2022.pdf](https://www.sbpr.org.br/site/media/arquivos/livro_de_resumos_ijc_radio_2022.pdf).
- [8] T. Scientific, “Radeye-prd alarming personal radiation detection”, EUA, Tech. Rep. DB-087-050322 E, 2008, p. 93.
- [9] J. S. Ribberink, J. J. van der Werf, T. O’Donoghue, *et al.*, “New practical model for sand transport induced by non-breaking waves and currents”, in *32nd International Conference on Coastal Engineering, ICCE 2010*, Coastal Engineering Research Council, 2011, pp. 1–14.
- [10] J. Kotowski, D. Olszewska-Nejbert, K. Nejbert, and M. Forster, “Long-distance transport of elastic material revealed by monazite and muscovite dating: Albian arenites, extra-carpathian poland”, *Sedimentary Geology*, vol. 446, p. 106 339, 2023.
- [11] J. Justo, V. Hamza, and F. Lamago Simões Filho, “Mobility of radionuclides during weathering and erosion in saquarema (rj): Implications for submerged monazite deposits in adjacent offshore areas.”, in *13th International Congress of the Brazilian Geophysical Society & EXPOGEF, Rio de Janeiro, Brazil, 26–29 August 2013*, Society of Exploration Geophysicists and Brazilian Geophysical Society, 2013, pp. 211–214.
- [12] M. Technologies, “Spir-id handheld detection identification”, EUA, Tech. Rep. d231e681-320a-4488-b639-f7faf119102b, 2006, p. 2.
- [13] G. E. Knoll, *Radiation Detection and Measurement*, 3rd ed. New York: John Wiley Sons, Inc., 1999, p. 816.
- [14] Scionix, “3”x3” bgo sipm scintillation detector with built in temperature compensated bias generator and preamplifier”, Holanda, Tech. Rep. 76B76<sub>S</sub>IP – E3 – BGO – X, 2021, p. 3.
- [15] N. Tsoulfanidis, *MEASUREMENT AND DETECTION OF RADIATION*, 4th ed. Boca Raton: CRC Press, 2015, p. 515.
- [16] A. M. Azevedo, D. D. Cardoso, M. P. C. Medeiros, S. Gavazza, and R. K. Morales, “Determination of steel and lead bi-laminated shielding for military vehicles”, *Brazilian Journal of Radiation Sciences*, vol. 11, no. 1A (Suppl.) Pp. 01–31, 2023.